1X

DECLASSIFIED

CONFIDENTIAL

NATIONAL AERONAUTICS AND SPACE ADMINISTRATION

TECHNICAL MEMORANDUM X-21

PRINCIPAL RESULTS FROM WIND-TUNNEL STABILITY TESTS OF SEVERAL PROPOSED SPACE CAPSULE MODELS UP TO AN ANGLE OF ATTACK OF 33°*

L
4
6
6

By Howard S. Carter, Ronald Kolenkiewicz,
and Roland D. English

SUMMARY

Several model configurations similar to the shape of a proposed space capsule were tested for reentry stability in five wind-tunnel facilities at the Langley Research Center. This report is a summary of the pertinent data from these tests.

The configurations had marginal static stability at low angles of attack for subsonic Mach numbers and somewhat higher static stability at all other angles of attack and Mach numbers of this investigation. Rounding the corners of the front face slightly at the edges had very little effect on the static stability but did reduce the streamwise forces slightly at some Mach numbers. At Mach numbers of 2.06 and 4.50, there was little or no effect of Reynolds number on the static stability. Dynamic tests using the forced-oscillation technique showed that the configuration was damped for all angles of attack and Mach numbers of this investigation. However, free-flight tests at a Mach number of 0.06 indicated steady-state oscillations with a magnitude of about ±45°.

INTRODUCTION

A program is under way at the Langley Research Center to develop a capsule configuration suitable for carrying man into space and return. As part of this program, proposed space capsule models were tested for static stability in the Langley 11-inch hypersonic tunnel, in the Langley Unitary Plan wind tunnel, and in the Langley 8-foot transonic pressure tunnel. A model was also tested for dynamic stability in the Langley 20-foot free-spinning tunnel and one was tested in the Langley transonic

*Title, Unclassified.

[redacted]

blowdown tunnel for damping in yaw. In all these tests, the models were positioned with their large blunt ends upstream since this is the attitude the capsule would be in during reentry.

This report is a summary of the pertinent data from these five tunnels pertaining to these capsule configurations as reentry vehicles. There are considerably more data available on the configurations discussed herein and on other closely allied configurations in references 1 to 4. In addition, several of the important body-shape parameters concerning the stability of blunt bodies during reentry are discussed in references 5 and 6.

SYMBOLS

C_A axial-force coefficient based on frontal area

C_D drag coefficient based on frontal area

C_L lift coefficient based on frontal area

C_{L_α} lift-curve slope per degree

C_m pitching-moment coefficient based on frontal area and diameter

C_{m_α} pitching-moment curve slope per degree

C_n yawing-moment coefficient based on frontal area and diameter

$C_{n_r} = \dfrac{\partial C_n}{\partial\left(\frac{rD}{2V}\right)}$ per radian

$C_{n_{\dot\beta}} = \dfrac{\partial C_n}{\partial\left(\frac{\dot\beta D}{2V}\right)}$ per radian

$C_{n_r} - C_{n_{\dot\beta}}$ total damping in yaw per radian

C_N normal-force coefficient based on frontal area

D frontal diameter, ft

M Mach number

N_{Re} free-stream Reynolds number based on frontal diameter

r yawing velocity, radians/sec

t time, sec

V velocity, ft/sec

α angle of attack, deg

β angle of sideslip, deg or radians

$\dot{\beta} = \frac{d\beta}{dt}$, radians/sec

ω angular frequency of oscillation, radians/sec

$\frac{\omega D}{2V}$ reduced frequency parameter, radians

L
4
6
6

FACILITIES AND MODELS

In figure 1 are presented sketches of the models showing pertinent dimensions and the facility or facilities in which each was tested. The models, even though of various diameters and various rear-end configurations, were closely similar in many respects. In order to show this similarity, the center-of-gravity locations and nose radii are shown in terms of the maximum diameter. The center-of-gravity locations varied from 0.29 body diameter to 0.31 diameter from the nose. The nose radius for all models was 1.5 diameters.

The model used in the 11-inch tunnel was sting supported. This was the original shape of the capsule configuration study reported herein. A description of the tunnel is presented in reference 7.

The model used in the spin tunnel was a somewhat later version of this capsule configuration. The model was completely free in the tunnel, the support being provided by the upgoing air.

The model as tested in the 26-inch transonic blowdown tunnel was closely similar to the spin-tunnel model except provision was made for a sting. This facility has the capability for determining both dynamic and static stability derivatives of models. For these tests, only the damping in yaw was determined. The mechanism used for these tests consisted of a sting-mounted model which was forced to perform a single-degree-of-freedom oscillation about its vertical axis. A description of the dynamic-stability mechanism and the principles involved are discussed in reference 8.

The two models tested in both the Langley 8-foot and the Langley Unitary Plan wind tunnels were also sting mounted. The two models were identical except for corner radius; one model had a sharp-edged corner and one had a 3/16-inch-radius corner. (See fig. 1.) The Langley Unitary Plan wind tunnel is described in reference 9.

TESTS

A list of the tests that were made in the various facilities is given in table I. In many of the tests, the Reynolds numbers approximated those of an actual trajectory for a full-scale capsule as it reentered the earth's atmosphere from a typical orbit. Figure 2 shows the Mach numbers and Reynolds numbers for a typical reentry trajectory of this capsule configuration. The tests in the Langley 8-foot tunnel were too low in Reynolds number at low subsonic speeds but did approximate the full-scale Reynolds numbers for the transonic speeds. Also, the tests in the Langley spin tunnel and in the Langley 11-inch hypersonic tunnel were made at Reynolds numbers less than those of the actual trajectory.

In order to determine the effect of Reynolds number on static stability, three tests were made in the Langley Unitary Plan wind tunnel at a Mach number of 2.06 and three tests at a Mach number of 4.50 for different Reynolds numbers. Two tests were made in the Langley transonic blowdown tunnel at a Mach number of about 0.61 to determine the effect of Reynolds number on the damping in yaw.

The tests in the 8-foot tunnel (ref. 4) were made over an angle-of-attack range of -3° to 20°. The tests in the Unitary Plan wind tunnel (ref. 3) covered an angle-of-attack range from about -4° to 184°. However, this report is a summary of data for the latter part of the reentry trajectory where model oscillations are limited, and only the data from -4° to 33° are presented. Likewise, the tests in the 11-inch tunnel (ref. 2) were made for an angle-of-attack range from 0° to 90°, but only the data from 0° to 30° are shown herein.

The model that was tested in the Langley 8-foot tunnel and in the Langley Unitary Plan wind tunnel was first tested with sharp corners for all Mach numbers shown. Then with the model corners rounded to

[redacted]

3/16-inch radius, the tests were repeated at all Mach numbers in the Langley 8-foot tunnel and at two Mach numbers in the Langley Unitary Plan wind tunnel.

RESULTS AND DISCUSSION

Static Tests

Figures 3 to 7 present the normal-force, axial-force, lift, drag, and pitching-moment coefficients as functions of angle of attack and Mach number. As discussed previously, the model that was tested in the Langley 8-foot tunnel and the Langley Unitary Plan wind tunnel was tested with both sharp corners and 3/16-inch-radius corners. For simplicity, only the data for the sharp-cornered models are faired in the figures. Practically no change was caused in the parameters C_N, C_L, and C_m due to this rounding of the corners. However, a small reduction in the streamwise forces C_A and C_D did occur at some Mach numbers.

Figure 3 shows a negative slope for the variations of normal-force coefficient with angle of attack near an angle of attack of 0°, for Mach numbers 1.14 and below. However, for these conditions the configuration had marginal static stability as shown by the pitching-moment curves in figure 7. Apparently, when the normal-force coefficient was negative, the center of pressure was forward of the center-of-gravity position.

The axial-force coefficient is presented in figure 4 as a function of angle of attack. This axial-force coefficient was essentially constant at each test Mach number for angles of attack up to 10°.

The curves of lift coefficient against angle of attack (fig. 5) had negative slopes up to an angle of attack of 30°. This effect was caused by the fact that the axial force on this configuration was much larger than the normal force and also by the fact that at some angles of attack and Mach numbers, the normal-force coefficient itself contributed to this negative slope. At angles of attack, therefore, this axial force had a larger component in the lift plane than did the normal force. This negative slope was as expected for high drag bodies.

The variation of pitching-moment coefficient with angle of attack is shown in figure 7 for all Mach numbers of the tests. These data indicate that the configuration had marginal static stability at low angles of attack for subsonic Mach numbers and somewhat higher static stability at all other angles of attack and Mach numbers at which tested.

In order to show the effect of Reynolds number on static stability, two additional tests were made at $M = 2.06$ and two at $M = 4.50$ at other Reynolds numbers. Figure 8 shows the variation of pitching-moment coefficient with angle of attack for these Reynolds number tests. Little or no effect of Reynolds number on $C_{m_{\alpha}}$ was obtained as is shown in figure 8(c). As in the previous figures, only the sharp-edged data are faired. The effect of rounding the corners at $M = 2.06$ appears to be negligible for the Reynolds numbers shown in figure 8(a).

The variation at an angle of attack of 0° of $C_{m_{\alpha}}$, $C_{L_{\alpha}}$, and C_D with Mach number is presented in figure 9. The data from the three tunnels faired together well. At or near a Mach number of 1.0, these parameters had a very decided change in their curves. The $C_{m_{\alpha}}$ curve indicated that the configuration had marginal static stability at all subsonic Mach numbers and somewhat higher static stability at supersonic speeds. These curves in figure 9 are not indicative of the data at other angles of attack because of the nonlinearities.

Dynamic Tests

A model was tested for dynamic stability in the Langley transonic blowdown tunnel by using the forced-oscillation technique. The model (fig. 1) was oscillated in yaw approximately $\pm 2.5^{\circ}$ at reduced frequencies $\frac{\omega D}{2V}$ of 0.02 to 0.03.

The damping-in-yaw data are presented in figure 10 in coefficient form $C_{n_r} - C_{n_{\dot{\beta}}}$ for angles of attack of 0°, 5°, and 10°. The data show that the configuration was damped for all angles of attack and Mach numbers at which tested. At an angle of attack of 0° a test was made at a different Reynolds number which showed a change in damping which was within the scatter of the data. Since the model was axially symmetric, this damping data for yaw at an angle of attack of 0° will also be the same as the damping in pitch.

This program for dynamic tests in the Langley transonic blowdown tunnel also included several other possible reentry shapes along with the one considered herein. These unpublished transonic data indicated that the damping characteristics of these blunt shapes were strongly influenced by the detailed flow conditions over the exposed surfaces. Since small changes in test conditions or in geometry of the model can change the damping considerably, model tests should be made as nearly similar as possible to the actual prototype.

In order to determine the dynamic stability of this configuration, it was tested in free flight in the spin tunnel at $M = 0.06$. The Reynolds numbers of these tests were very low in comparison to those for an actual reentry capsule. Also the inertia of the model was not to scale. The only data obtained were model behavior from motion pictures. Hence, only qualitative conclusions were obtained.

For these tests, the model was released in the spin tunnel in a random attitude. Regardless of its initial attitude, the model settled down to an amplitude of oscillations of about $\pm 45^{\circ}$ and maintained these sizable oscillations for the duration of each test.

SUMMARY OF RESULTS

Models of a proposed capsule suitable for carrying man into space and return were tested for reentry stability in five tunnels at the Langley Research Center. The following results were obtained:

1. The configurations had marginal static stability at low angles of attack for subsonic Mach numbers and somewhat higher static stability at all other angles of attack and Mach numbers of this investigation.

2. The static stability was affected negligibly by changing the corners at the edges of the front face from a sharp edge to a 3/16-inch radius. A small reduction in the streamwise axial-force and drag coefficients did occur, however, at some Mach numbers.

3. At Mach numbers of 2.06 and 4.50, there was little or no effect of Reynolds number on the static stability of this configuration.

4. The damping-in-yaw tests with the forced-oscillation technique showed that the configuration was damped for all angles of attack and Mach numbers of this investigation.

5. The axial force on the blunt model was essentially constant at each test Mach number for angles of attack up to about 10°.

6. Free-flight tests in the Langley 20-foot free-spinning tunnel at a Mach number of 0.06 indicated steady-state oscillations with a magnitude of about $\pm 45^{\circ}$.

Langley Research Center,
National Aeronautics and Space Administration,
Langley Field, Va., March 31, 1959.

REFERENCES

1. Bird, John D., and Reese, David E., Jr.: Stability of Ballistic Reentry Bodies. NACA RM L58E02a, 1958.

2. Penland, Jim A., and Armstrong, William O.: Preliminary Aerodynamic Data Pertinent to Manned Satellite Reentry Configurations. NACA RM L58E13a, 1958.

3. Turner, Kenneth L., and Shaw, David S.: Wind-Tunnel Investigation at Mach Numbers From 1.60 to 4.50 of the Static-Stability Characteristics of Two Nonlifting Vehicles Suitable for Reentry. NASA MEMO 3-2-59L, 1959.

4. Pearson, Albin O.: Wind-Tunnel Investigation at Mach Numbers From 0.40 to 1.14 of the Static Aerodynamic Characteristics of a Nonlifting Vehicle Suitable for Reentry. NASA MEMO 4-13-59L, 1959.

5. Fisher, Lewis R., Keith, Arvid L., Jr., and Dicamillo, Joseph R.: Aerodynamic Characteristics of Some Families of Blunt Bodies at Transonic Speeds. NASA MEMO 10-28-58L, 1958.

6. Allen, H. Julian: Motion of a Ballistic Missile Angularly Misalined With the Flight Path Upon Entering the Atmosphere and Its Effect Upon Aerodynamic Heating, Aerodynamic Loads, and Miss Distance. NACA TN 4048, 1957. (Supersedes NACA RM A56F15.)

7. McLellan, Charles H., Williams, Thomas W., and Bertram, Mitchel H.: Investigation of a Two-Step Nozzle in the Langley 11-Inch Hypersonic Tunnel. NACA TN 2171, 1950.

8. Braslow, Albert L., Wiley, Harleth G., and Lee, Cullen Q.: Dynamic Directional Stability Derivatives for a 45° Swept-Wing—Vertical-Tail Airplane Model at Transonic Speeds and Angles of Attack, With a Description of the Mechanism and Instrumentation Employed. NACA RM L58A28, 1958.

9. Anon.: Manual for Users of the Unitary Plan Wind Tunnel Facilities of the National Advisory Committee for Aeronautics. NACA, 1956.

L-466

TABLE I.- TEST PARAMETERS

Static tests			
Facility	M	N_{Re}	α, deg
Langley 8-foot transonic pressure tunnel	0.40	2.01×10^6	-3 to 20
	.60	2.75	-3 to 20
	.80	3.28	-3 to 20
	.90	3.45	-3 to 20
	.95	3.50	-3 to 20
	1.00	3.60	-3 to 20
	1.03	3.63	-3 to 20
	1.14	3.64	-3 to 20
Langley Unitary Plan wind tunnel	2.06	0.88×10^6	-4 to 31
	2.06	1.75	-4 to 31
	2.06	2.62	-4 to 31
	2.87	2.62	-4 to 32
	3.39	3.41	-4 to 32
	3.90	3.41	-4 to 32
	4.50	1.75	-4 to 33
	4.50	3.41	-4 to 33
	4.50	5.06	-4 to 33
Langley 11-inch hypersonic tunnel	6.86	0.25×10^6	0 to 30

Dynamic tests					
Facility	M	N_{Re}	α, deg	β, deg	$\frac{\omega D}{2V}$
Langley 20-foot free-spinning tunnel	0.060	0.25×10^6	Free to oscillate	Free to oscillate	-----
Langley transonic blowdown tunnel	0.606	6.5×10^6	0	-2.5 to 2.5	0.017
	.616	3.2	0	-2.5 to 2.5	.027
	.703	3.2	0	-2.5 to 2.5	.026
	.809	3.2	0	-2.5 to 2.5	.023
	.917	3.2	0	-2.5 to 2.5	.020
	.919	3.2	0	-2.5 to 2.5	.021
	.994	3.2	0	-2.5 to 2.5	.021
	1.005	3.2	0	-2.5 to 2.5	.021
	.621	3.2	5	-2.5 to 2.5	.018
	.813	3.2	5	-2.5 to 2.5	.023
	.824	3.2	5	-2.5 to 2.5	.023
	.895	3.2	5	-2.5 to 2.5	.022
	.922	3.2	5	-2.5 to 2.5	.022
	.982	3.2	5	-2.5 to 2.5	.021
	1.005	3.2	5	-2.5 to 2.5	.021
	.617	3.2	10	-2.5 to 2.5	.030
	.621	3.2	10	-2.5 to 2.5	.029
	.696	3.2	10	-2.5 to 2.5	.028
	.704	3.2	10	-2.5 to 2.5	.027
	.801	3.2	10	-2.5 to 2.5	.024
	.905	3.2	10	-2.5 to 2.5	.023
	.998	3.2	10	-2.5 to 2.5	.022
	1.003	3.2	10	-2.5 to 2.5	.022

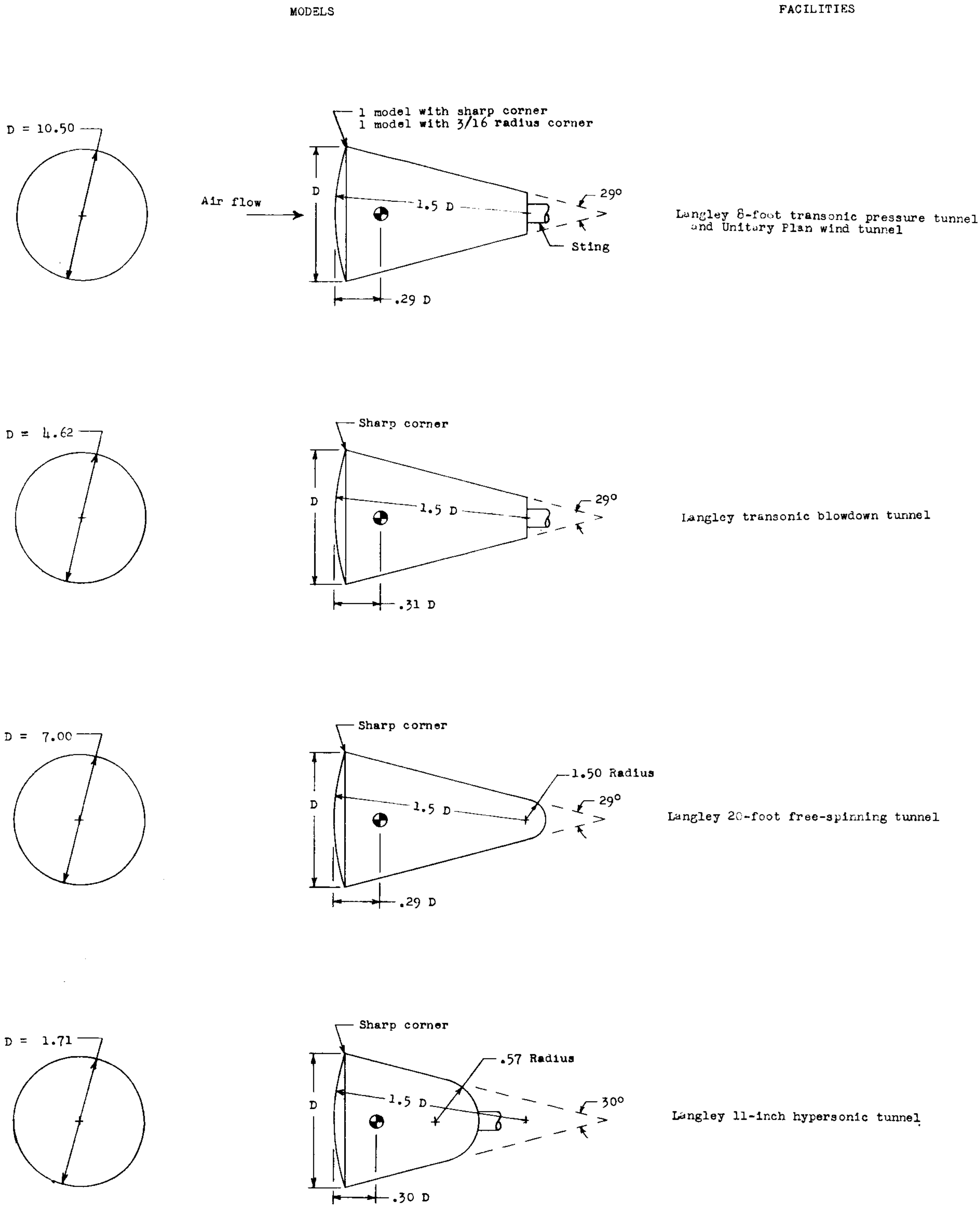

Figure 1.- Sketches of the models showing pertinent dimensions and the facility or facilities in which each was tested. All dimensions are in inches.

[redacted]

L-466

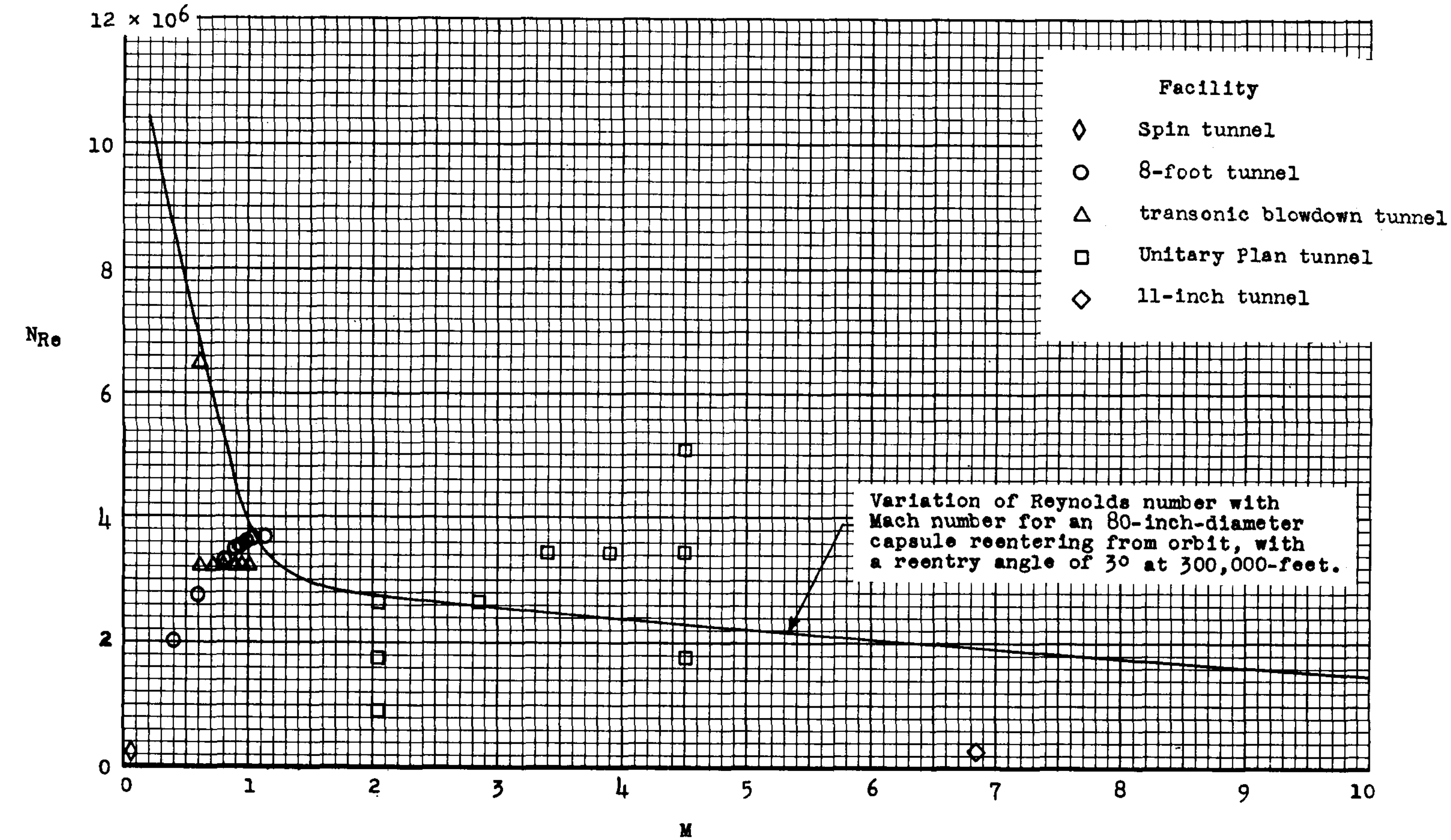

Figure 2.- Comparison of the Reynolds numbers of the tests to those of a calculated reentry trajectory for the full-scale model.

L-466

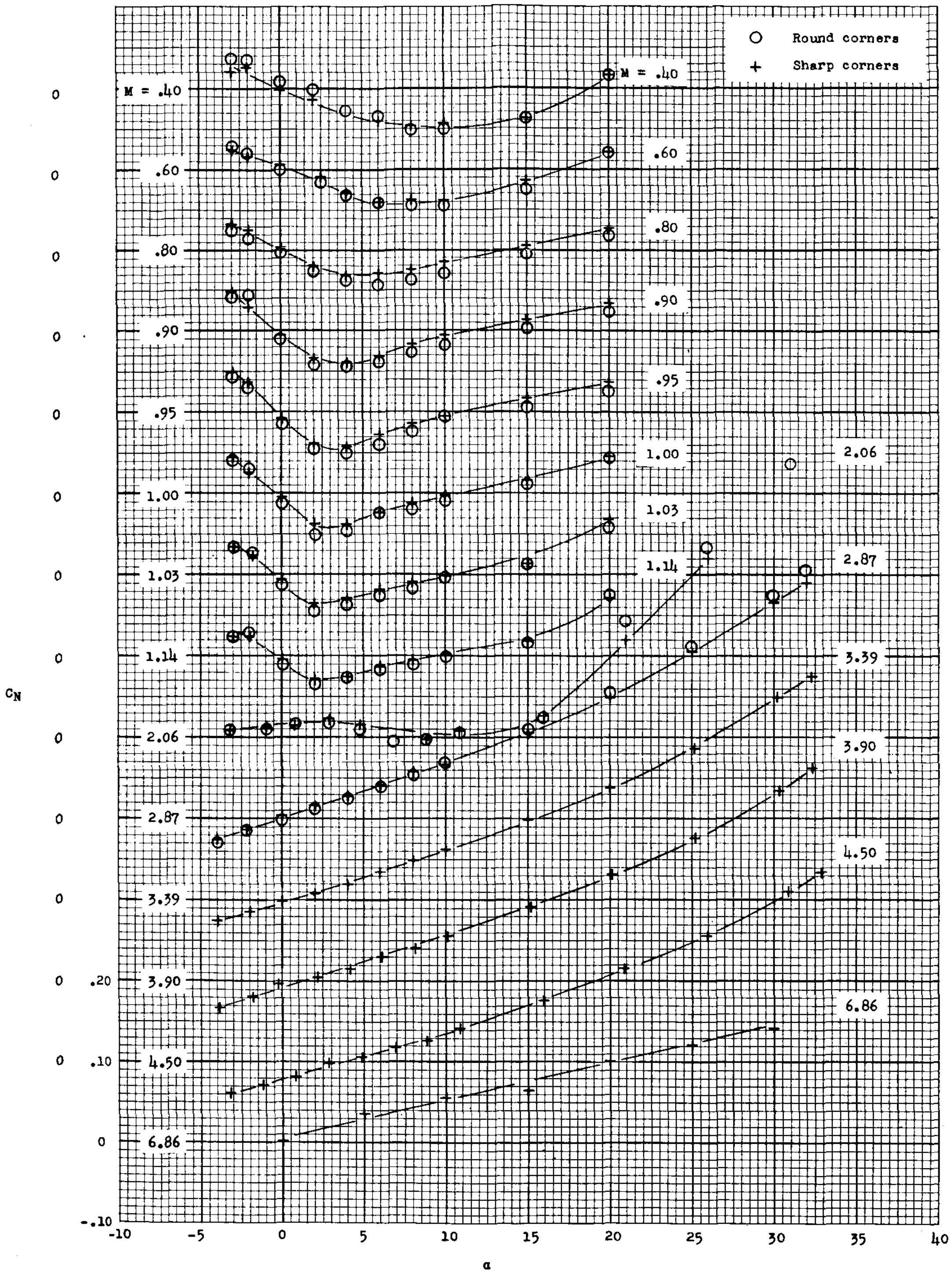

Figure 3.- Variation of normal-force coefficient with angle of attack for various Mach numbers.

[redacted]

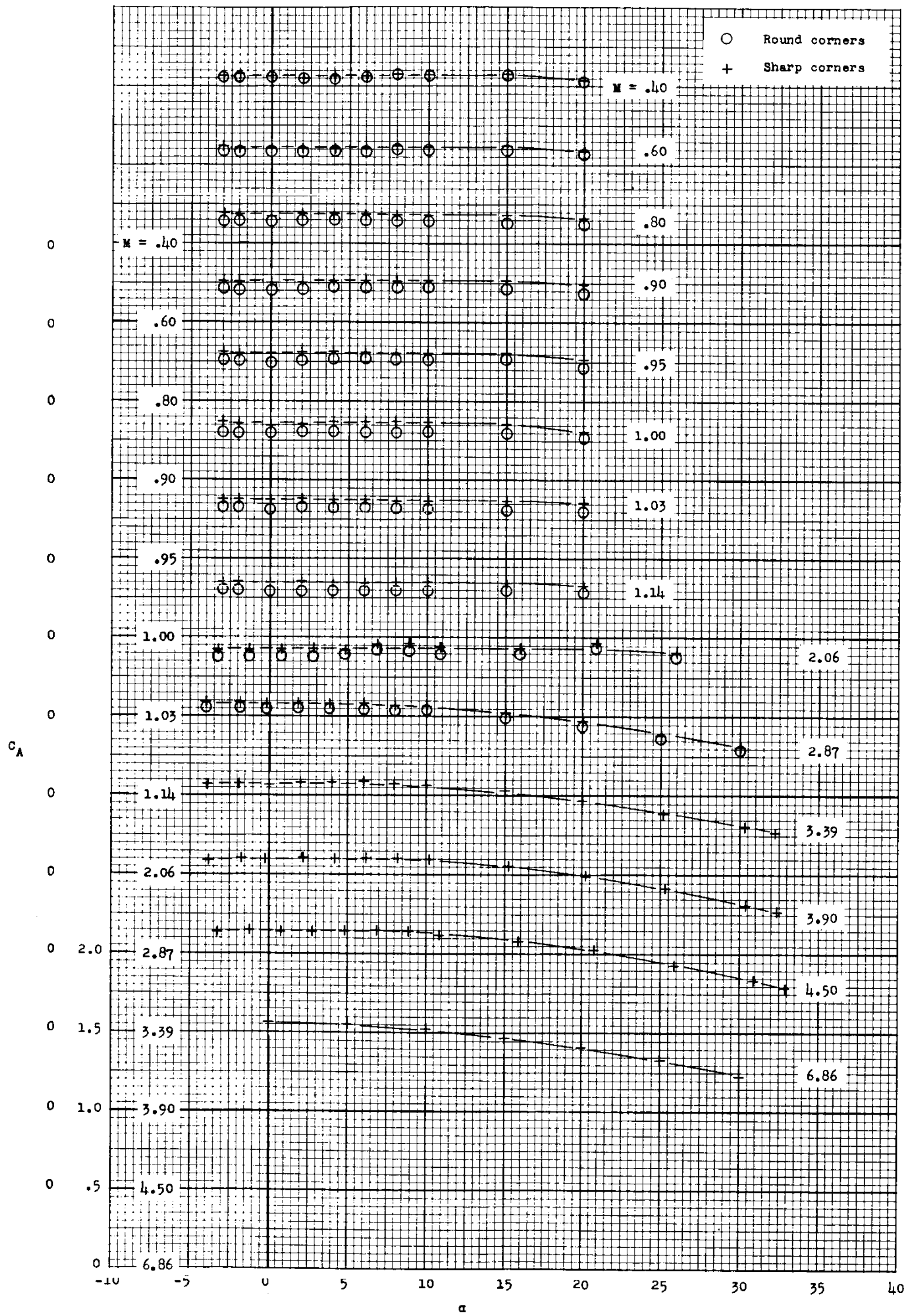

Figure 4.- Variation of axial-force coefficient with angle of attack for various Mach numbers.

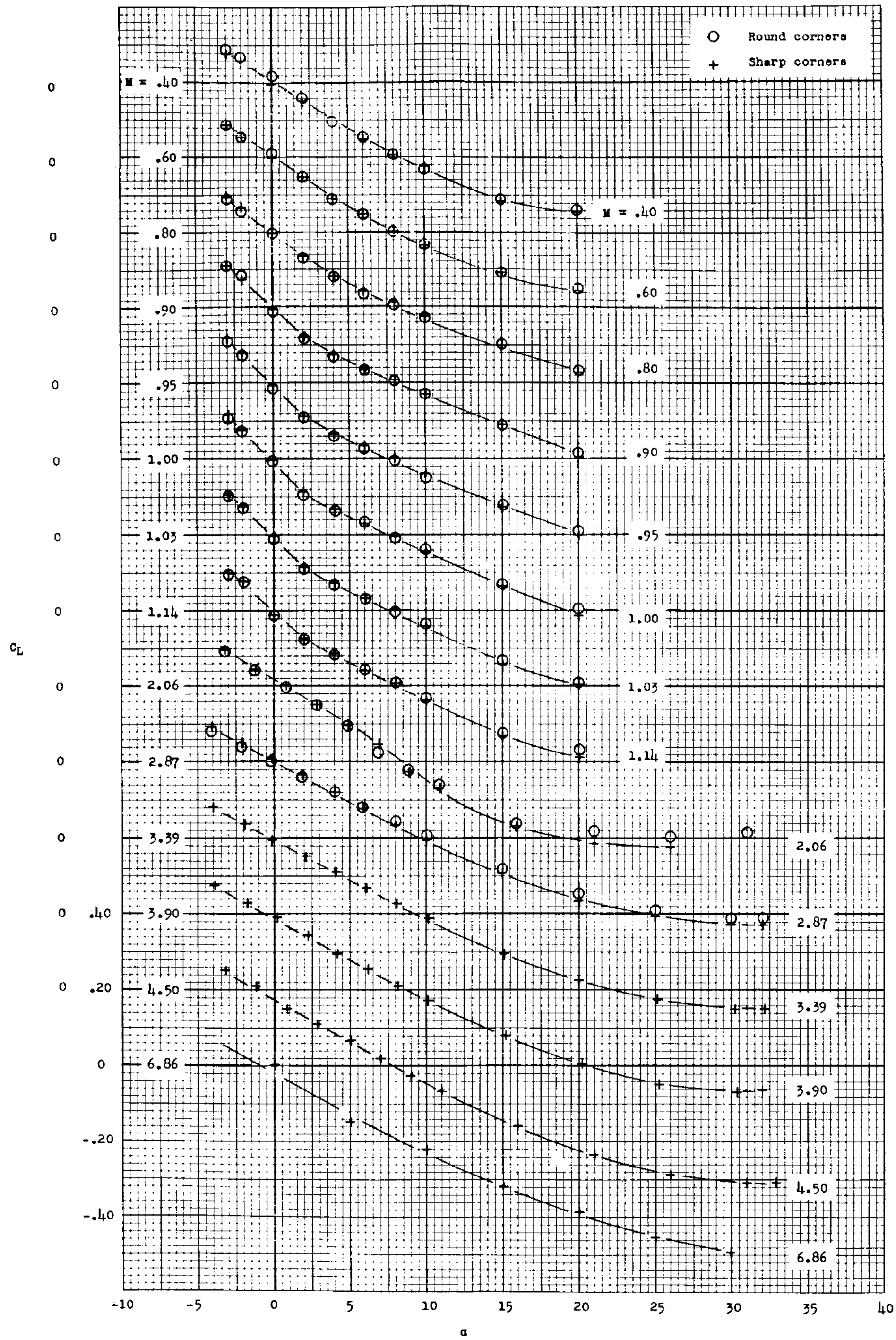

Figure 5.- Variation of lift coefficient with angle of attack for various Mach numbers.

[redacted]

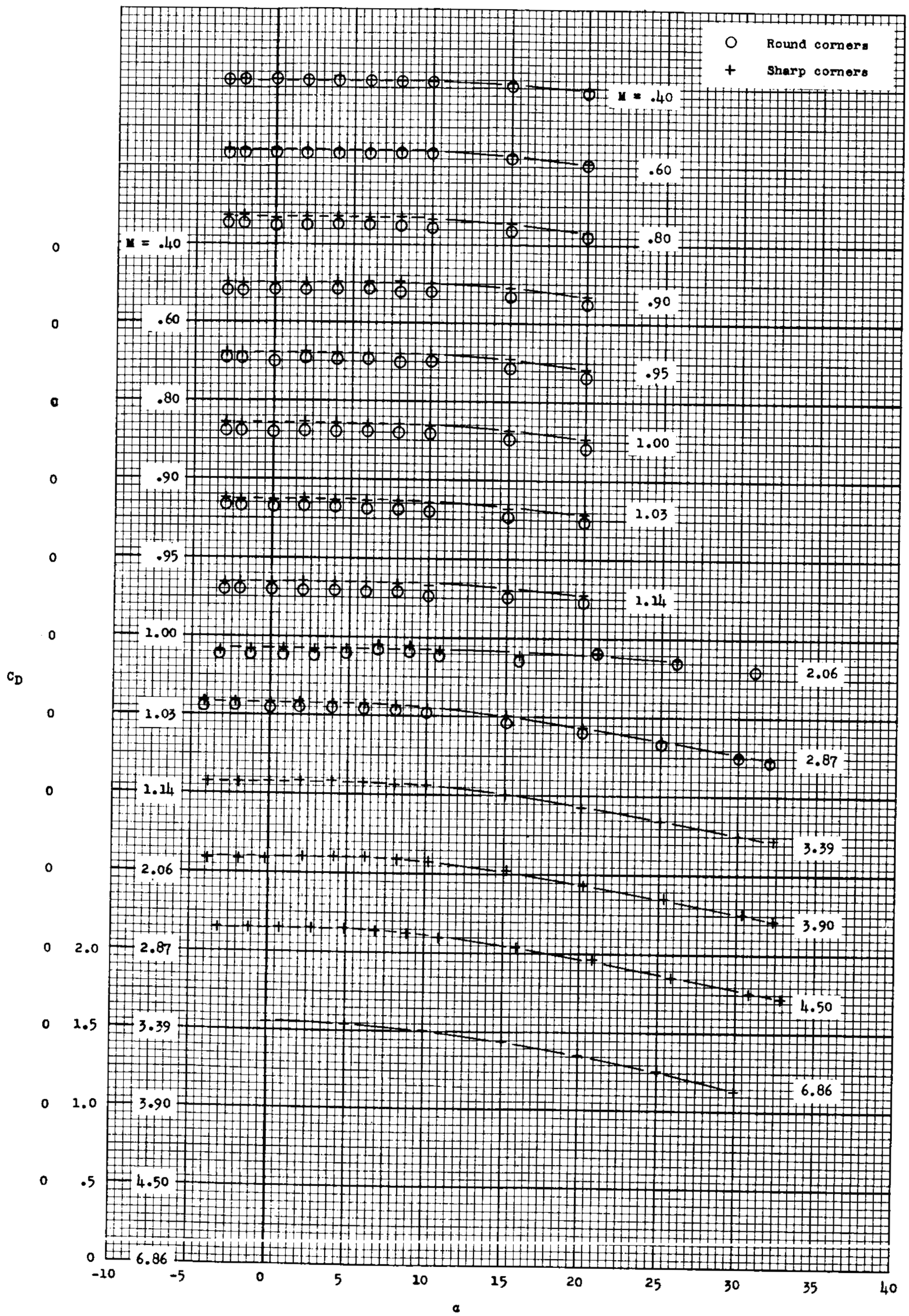

Figure 6.- Variation of drag coefficient with angle of attack for various Mach numbers.

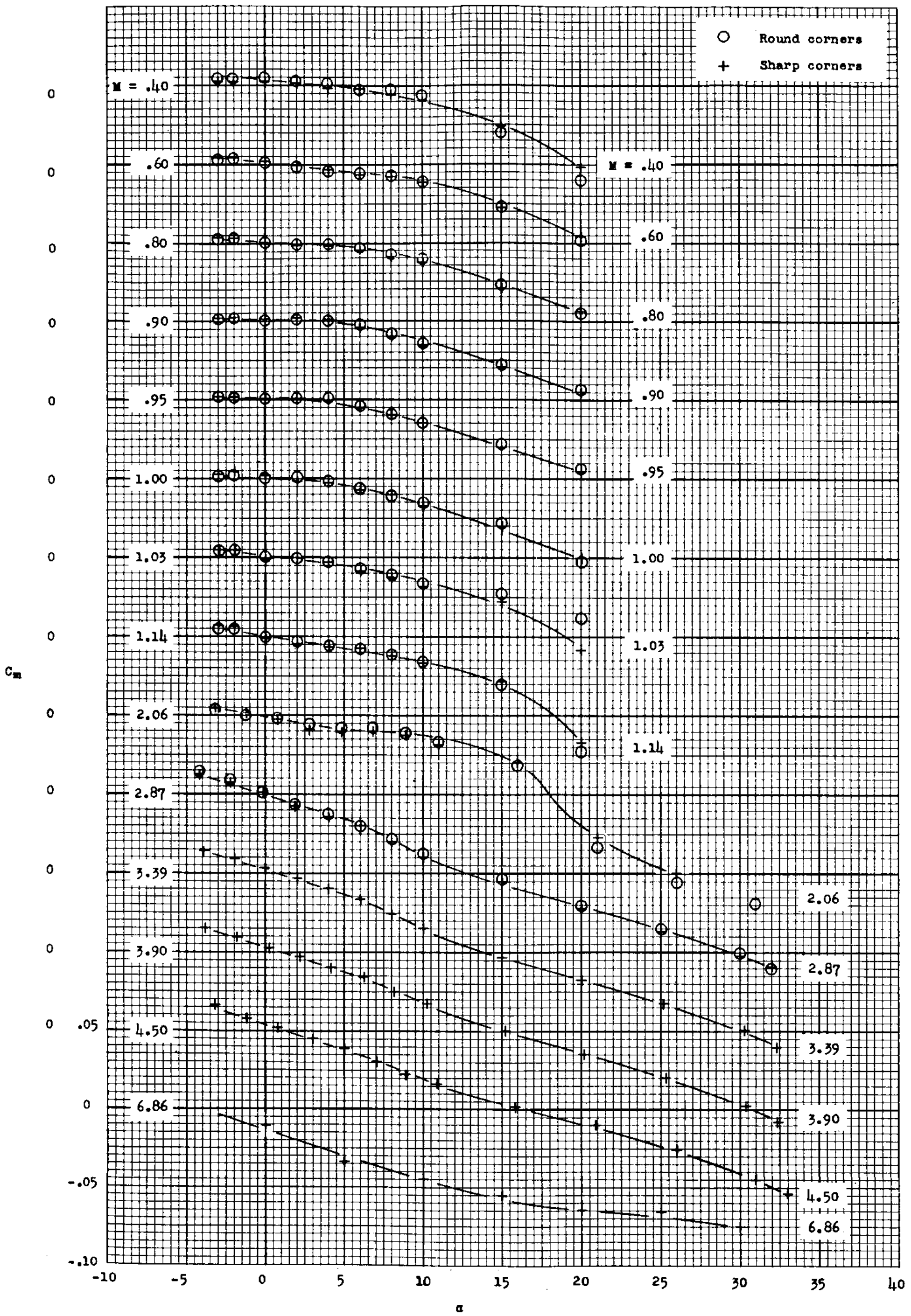

Figure 7.- Variation of pitching-moment coefficient with angle of attack for various Mach numbers.

[redacted]

L-466

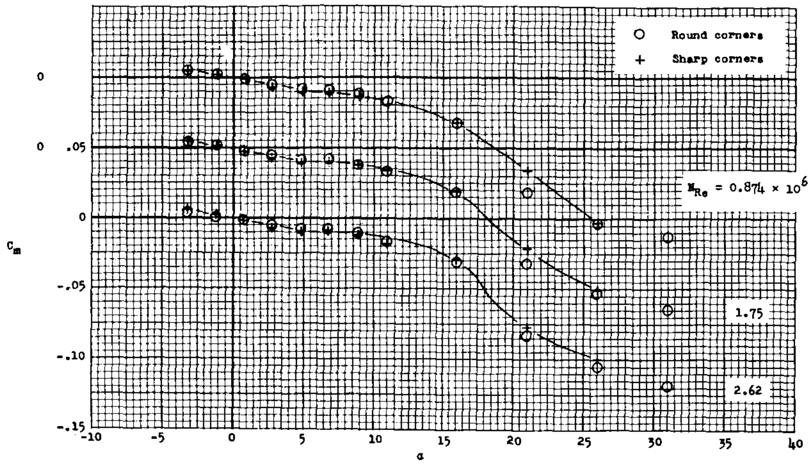

(a) Variation of pitching-moment coefficient with angle of attack for three Reynolds numbers. M = 2.06.

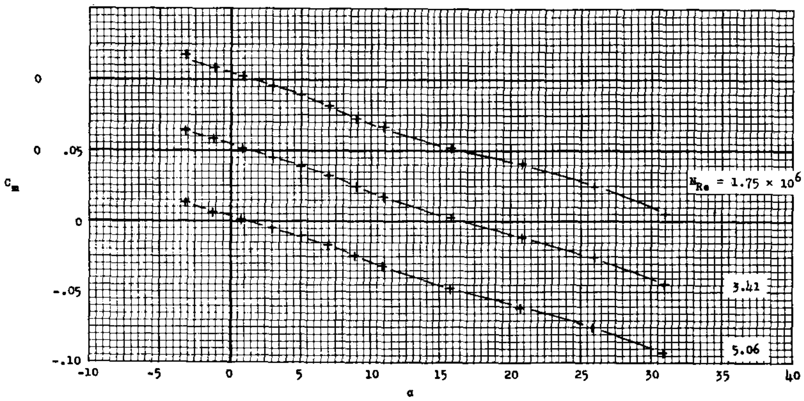

(b) Variation of pitching-moment coefficient with angle of attack for three Reynolds numbers. M = 4.50.

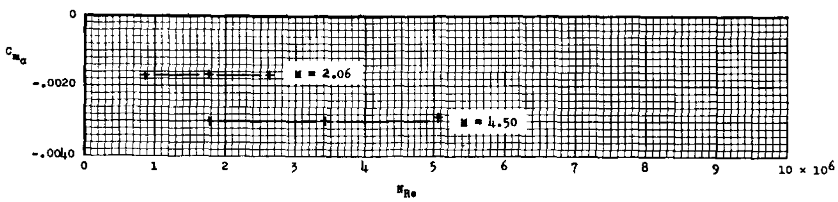

(c) Variation of C_{m_α} at zero angle of attack with Reynolds number for M = 2.06 and 4.50.

Figure 8.- Effect of Reynolds number on static stability at M = 2.06 and 4.50.

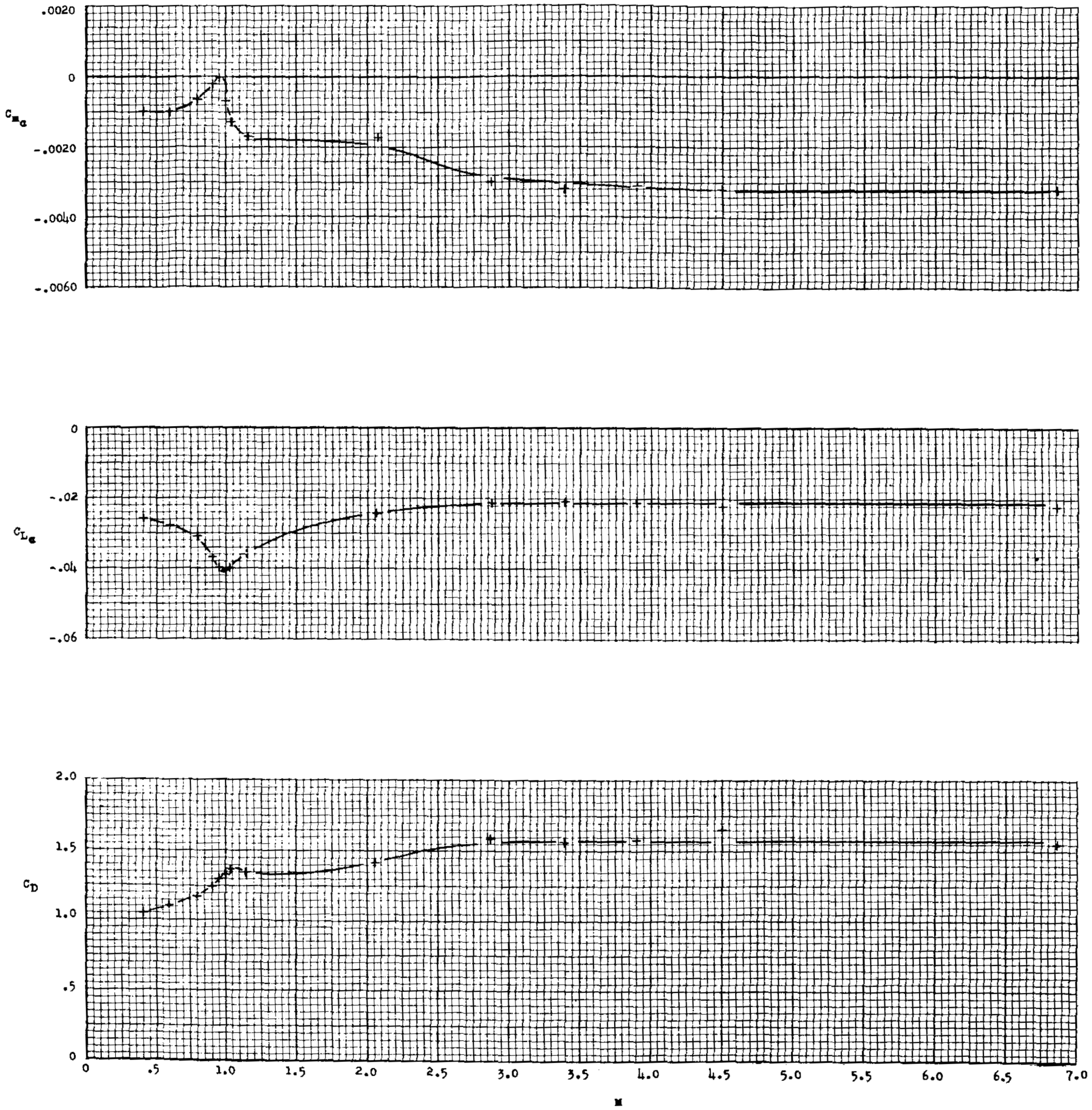

Figure 9.- Variation at an angle of attack of 0° of C_{m_α}, C_{L_α}, and C_D with Mach number.

[redacted]

L-466

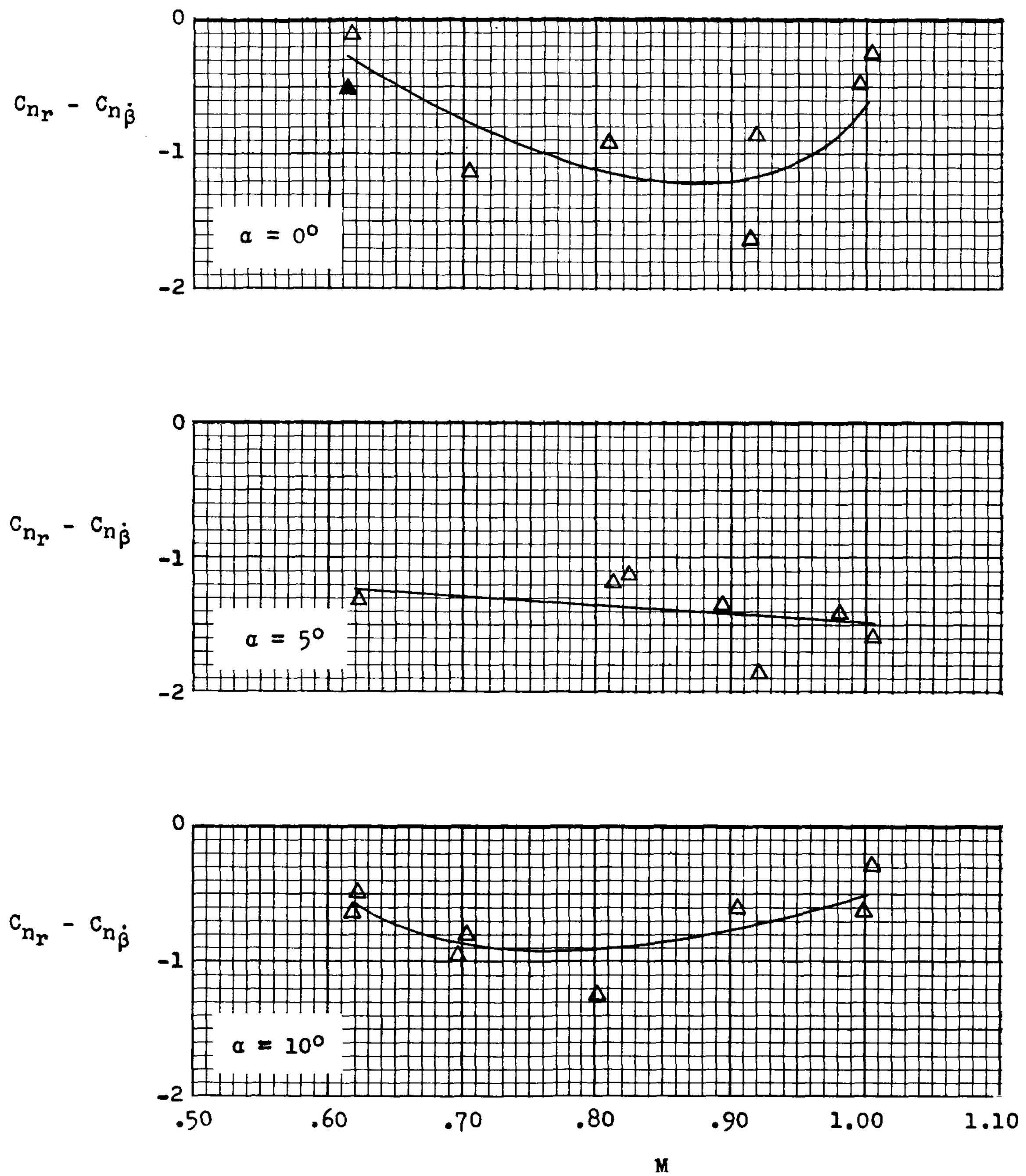

Figure 10.- Variation of damping in yaw with Mach number and angle of attack. $\frac{\omega D}{2V} = 0.02$ to 0.03. Transition fixed. Reynolds number was 3.2×10^6 for open symbols and 6.5×10^6 for solid symbols.